Progress In Electromagnetics Research B, Vol. 29, 269–288, 2011

NEW TECHNIQUES FOR INCREASING ANTENNA BANDWIDTH WITH IMPEDANCE LOADING

R. A. Formato

Registered Patent Attorney & Consulting Engineer
Cataldo & Fisher, LLC
400 Trade Center, Suite 5900 Woburn, MA 01801, USA

Abstract—New methods are presented for increasing the bandwidth of wire antennas using impedance loading. This paper extends the seminal Wu-King theory of the internal impedance profile that produces travelling-wave only current modes on a center-fed dipole antenna. It also presents a numerical optimization methodology based on Central Force Optimization, a new deterministic multidimensional search and optimization metaheuristic useful for problems in applied electromagnetics. A CFO-optimized loaded monopole antenna is described in detail and compared to the same structure loaded with a fractional Wu-King profile. The CFO monopole generally performs better than other designs using either the full or fractional Wu-King profiles or the extended Wu-King profiles. The methods described in this paper should be useful in any wire antenna design that utilizes impedance loading to increase bandwidth.

1. INTRODUCTION

This paper describes two methods for increasing wire antenna bandwidth using impedance loading: (1) an extension of the seminal analytic Wu-King loading profile, and (2) a numerical approach based on Central Force Optimization. The notion of increasing antenna bandwidth by adding impedance loading has been around for long time, at least since the early 1950s. In 1953, for example, Willoughby published his Patent Specification for "An Improved Wide Band Aerial" [1]. It discloses wire antenna elements that include a multiplicity of individual resistors, or wire segments with different conductivity, whose resistance values increase exponentially with distance from the radio-frequency (RF) source.

Received 19 February 2011, Accepted 6 April 2011, Scheduled 8 April 2011
Corresponding author: Richard A. Formato (rf2@ieee.org).

In 1961, Altshuler described a "Traveling-Wave Linear Antenna" [2] whose input impedance was essentially constant over an octave in frequency. The flat response resulted from inserting a $240\,\Omega$ resistor one-quarter wavelength ($\lambda/4$) from the end of a wire radiating element. Altshuler determined the value and location of the loading resistance by analogizing the antenna to an open-ended transmission line. His analysis is based on the relationship between a line's characteristic impedance, Z_0, and a wire antenna's expansion parameter Ψ. Physically, Ψ represents the ratio of the antenna's surface vector potential to its axial current, and is approximately constant along the radiator as long as the current is not too small. For a dipole of half-length h and radius a, $\Psi \approx 2[\ln(\frac{2h}{a}) - 1]$, and the corresponding loading resistance that produces an approximately travelling wave current distribution is on the order of 60Ψ ohms.

Altshuler's initial work on resistive loading was extended by Wu and King (WK) in a seminal paper published in 1965 [3]. Instead of using a single lumped resistance, WK assumed a continuously variable resistance along a center-fed dipole (CFD) antenna. The objective of their analysis was to determine an impedance loading profile that resulted in a purely travelling wave current mode. The WK profile has been the basis of most if not all subsequent work on impedance-loaded wire elements.

The performance achieved by continuously loaded antennas over the years has been impressive. For example, Kanda [4] built a small receive-only loaded-CFD field probe using the full WK profile that exhibited essentially flat response from HF to beyond 1 GHz. Both resistive and capacitive loading were employed by depositing a segmented, conductive thin-film of varying thickness on a glass rod substrate. Reactive loading was achieved by burning away with a laser narrow rings between conductive segments. Unfortunately, this field sensor was so heavily loaded that its radiation efficiency was far too low for use as a transmit antenna (transfer function typically below $-22\,\mathrm{dB}$). The full WK profile tends to load the antenna very heavily with an attendant substantial reduction in radiation efficiency.

This issue was addressed by Rama Rao and Debroux (RD), who designed, fabricated and measured a continuously loaded high frequency (HF) monopole [5, 6]. Because the full WK profile generally results in poor efficiency, the RD monopole used a fractional loading profile equal to 0.3 times the Wu-King profile ("30% profile"), along with a fixed, lumped-element matching network. Besides fractional profiles, other loading profiles have been proposed that combine resistance and inductance to improve bandwidth and efficiency [7]. Recently, Lestari et al. revisited the WK analysis in order to develop an

optimal linear loading profile for a ground penetrating radar bow-tie antenna [8]. Additional analyses of dipole structures generally appear in [9–12].

This paper describes a modification to the WK profile that results in higher radiation efficiency by increasing the average antenna current while maintaining the traveling-wave current mode necessary for increased bandwidth. Because the fields radiated by an antenna are proportional to its Idl product (current moment), increasing the average current increases the radiated fields, which, in turn, improves efficiency. The current distribution produced by the WK loading profile decays linearly along the antenna. The improved profile produces a traveling-wave current mode with a power law decay, of which the WK profile is a special case.

This paper is organized as follows: Section 2 presents an overview of the Wu-King theory, while Section 3 describes the extension of that theory. The extended theory is applied to the RD HF monopole as a design example in Section 4. Section 5 applies Central Force Optimization to the loaded monopole problem and compares its results to the performance of the analytic loading profiles. Section 6 is the conclusion.

2. WU-KING THEORY

The WK model assumes that the CFD has an internal impedance profile along the wire element given by $Z^i(z) = R^i(z) + jX^i(z)$, where $Z^i(z)$ is the (complex) internal impedance per unit length (ohms/meter) consisting of lineal resistance $R^i(z)$ and reactance $X^i(z)$ with $j = \sqrt{-1}$. z is the distance from the RF source. WK develops the differential equation satisfied by the CFD's current $I_z(z)$ and then determines by inspection that a traveling-wave current mode exists for one particular impedance profile Z^i.

The WK current distribution is $I_z(z) \approx (1 - \frac{|z|}{h}) \exp(-j\,k_0\,|z|\,)$, which consists of the product of a linearly decreasing ("straight line") amplitude factor $(1 - \frac{|z|}{h})$ and a traveling wave propagation factor in the complex exponential term $\exp(-j\,k_0|z|)$. $k_0 = 2\pi/\lambda_0$ is the wavenumber. The propagation factor represents a current wave progressing outward along each dipole arm. There is no reflected wave propagating toward the source to form a standing wave pattern, and consequently no resonance effect.

This current distribution exists only when the CFD element has a specific "$1/z$" internal impedance profile. The required profile is given by $Z^i(z) = \frac{60(\Psi/h)}{1-\frac{|z|}{h}}$, where $\Psi = \Psi_R + j\Psi_I$ is the complex expansion

parameter [2, 3] with real and imaginary parts subscripted R and I, respectively. Ψ is the ratio of the antenna element's surface vector potential to axial current, and is approximately constant along its length. The $1/z$ profile is the basis for the resistive loading used in [4–7].

The expansion parameter is defined as [3]

$$\Psi = 2\left[\sinh^{-1}\left(\frac{h}{a}\right) - C(2k_0a, 2k_0h) - jS(2k_0a, 2k_0h)\right] + \frac{j}{k_0h}\left[1 - \exp\left(-j2k_0h\right)\right].$$

C and S are the generalized sine and cosine integrals [3, 13] given by $C(b,x) = \int_0^x \frac{1-\cos(W)}{W}du$, $S(b,x) = \int_0^x \frac{\sin(W)}{W}du$, $W = \sqrt{u^2+b^2}$.

Because Ψ is frequency dependent, it usually is evaluated at the antenna's fundamental half-wave resonance, that is, $\lambda_0 = 4h$ (see [3] for details). As discussed below, however, this choice is not necessarily the best. Of course, the design frequency f_0 (Hz) at which Ψ is evaluated and the corresponding wavelength λ_0 (meters) are related by $f_0\,\lambda_0 = c \approx 2.998 \times 10^8$ m/s where c is the free-space velocity of light. Note that the design frequency f_0 for evaluating Ψ is not the RF source frequency.

3. IMPROVED ANALYTIC LOADING PROFILE

The WK $1/z$ profile is a special case of a more general profile that results in higher radiation efficiency. The first step in deriving the generalized profile is to assume a power law traveling-wave current distribution. The next step is to substitute this assumed current distribution into the current equation developed by WK, which then yields the condition that must be satisfied by the element's internal impedance in order to generate traveling-wave-only modes. This approach is fundamentally different than in [3] because the loading profile for a particular traveling-wave current mode now is an unknown which is determined by solving the appropriate equations.

The generalized CFD current distribution is assumed to be of the form $I_z(z) = C(h-|z|)^{\nu}\exp(-jk_0|z|)$ where C is a complex constant determined by the current at the feed point. Instead of the WK linear decay, the current amplitude now decays with a power law variation $(h-|z|)^{\nu}$ with exponent ν (profile exponent). As in [3], $\exp(-jk_0|z|)$ is the travelling wave propagation factor. When $\nu = 1$ the Wu and King case is recovered, but when $\nu \neq 1$ the more general case is obtained. Figure 1 shows typical current amplitude distributions parametric in the profile exponent ν, I_0 being the CFD's feed point current. It is

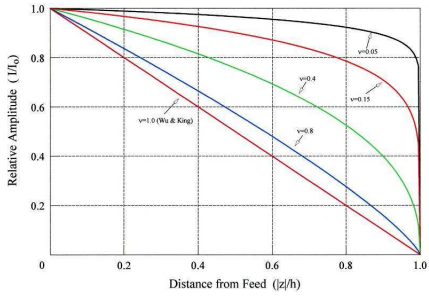

Figure 1. CFD current distributions parametric in profile exponent ν.

apparent that values of ν less than unity create significantly higher average antenna currents. Radiating elements with these current distributions are more efficient than those using the $1/z$ loading profile corresponding to $\nu = 1$.

The improved internal impedance profile is determined as follows. The derivatives $\frac{dI_z}{dz}$ and $\frac{d^2I_z}{dz^2}$ are computed and substituted into the equation satisfied by $I_z(z)$, Equation (11) in [3]. The resulting equation is satisfied by the auxiliary function $f(z)$ introduced in Equation (9) in [3]. The solution for $f(z)$ is $f(z) = 2\nu(h-|z|)^{\nu-2}\{1 - j\frac{\nu-1}{2k_0(h-|z|)}\}$, which generalizes Equation (12) in [3] and recovers it when $\nu = 1$. The extended impedance profile that produces travelling-wave-only modes is determined by $f(z)$.

The loading profile resistance and reactance per unit length (units of ohms/meter) are computed from $f(z)$ to be

$$R^i(z) = 60\nu(h-|z|)^{\nu-2}\left\{\Psi_R - \frac{(1-\nu)\Psi_I}{2k_0(h-|z|)}\right\} \tag{1a}$$

$$X^i(z) = 60\nu(h-|z|)^{\nu-2}\left\{\Psi_I + \frac{(1-\nu)\Psi_R}{2k_0(h-|z|)}\right\} \tag{1b}$$

The corresponding lineal inductance (henrys/meter) or capacitance (farads/meter) are $L^i = X^i/\omega_0$ and $C^i = 1/(\omega_0 X^i)$, respectively, for $X^i \geq 0$ and $X^i < 0$. The circular frequency is $\omega_0 = 2\pi f_0$ where f_0 is the design frequency (Hz) at which Ψ is computed. While f_0 usually is the antenna's half-wave resonant frequency, this is not necessarily the best choice as discussed in [14, 15].

The improved loading profile in Equation (1) above contains both resistance and reactance. But many practical designs employ only resistive loading because excellent results often are achieved even without the reactive component (see [5, 6], for example). In the monopole antenna designs discussed below only resistive loading is considered.

4. LOADED HF MONOPOLE USING ANALYTIC PROFILE

Rama Rao and Debroux's work provides a useful analytical and experimental benchmark for testing the improved loading profile. They designed, fabricated and measured a 35-foot tall, 2-inch diameter, continuously resistively loaded base-fed monopole antenna using full and fractional WK profiles. The loading profile was computed using WK theory and the antenna performance modeled with the NEC Method of Moments code version 3 (see below). The antenna then was built using different loading profiles, and extensive measurements were made of its performance [5, 6]. The measured RD data validated both the WK model and NEC's results, to quote, "The input impedance values predicted by both theories are in good qualitative agreement with the measured results and confirm the non-resonant behavior of the antenna." [5, p. 1226].

NEC-modeled monopole performance thus agrees well with measured data, thereby validating NEC as an accurate predictive tool for loaded wire element antenna design. The results reported here also are computed using NEC; but, instead of the RD loading profiles, new profiles are applied using the extended WK theory and a numerical optimization algorithm. This paper therefore compares its analytical results directly to RD's analytical results through the NEC modeling engine. This paper does not, however, report new measurement results using the modified loading profiles because, based on how well the RD measured and NEC-computed data agree, there is no reason even to suspect that NEC does not accurately calculate the monopole's performance.

The objectives of the RD design were (1) as flat as possible an impedance bandwidth and (2) a stable radiation pattern at low take-off angles to support long range HF links from 5 to 30 MHz. A continuously varying resistance along the antenna was created by coating a dielectric substrate with variable thickness chromium film. The RD design resulted in a voltage standing wave ratio (VSWR) $\leq 2:1$ relative to $50\,\Omega$ and radiation efficiency in the range 15%–36%. Because VSWR fluctuated substantially, achieving the VSWR objective required the use of a 6-element matching network and $4:1$ transformer, a tradeoff that appears to be typical. As the impedance response is progressively flattened in a loaded antenna, the radiation efficiency drops, often precipitously, and vice versa. The improved loading profile described here mitigates this effect.

Equation (1) above was used to compute a discrete resistance-only loading profile for the RD monopole geometry, that is, a base-

fed element $h = 10.668$ meters tall, $a = 0.0254$ meters radius on a PEC (perfectly electrically conducting) ground plane. Because single-element lumped resistances are used, a filamentary antenna wire could be used instead of the 2-inch diameter substrate. But the same geometry as the RD monopole was modeled because the antenna's length-to-diameter ratio does influence its bandwidth, although in this case the effect is minor (a maximum bandwidth metallic monopole element has $h \sim 10a$ [16]).

The fundamental half-wave resonance of 7.028 MHz was used as the design frequency. The generalized sine/cosine integrals were numerically evaluated using 32-point Gauss quadrature (see generally [13]). The antenna was modeled with NEC-2D (Numerical Electromagnetics Code Version 2 Double Precision), which was used because it is freely available online [17]. NEC's modeling guidelines and the model validation procedure described in [18, 19] were followed, and as a check the antenna was modeled with the most recent version of NEC as well (NEC-4.1D). Both versions of NEC yield essentially the same results.

Fourteen equal-length segments were used with each segment loaded at its midpoint using NEC "LD" cards. The loading resistance value was calculated segment-by-segment as $R_L^k = R^i(z_k^c) \cdot \Delta$, $k = 1, \ldots, 14$ where $\Delta = h/14$ is the constant segment length and $z_k^c = (2k-1)\frac{\Delta}{2}$ is the z coordinate at the center of the kth segment. A typical NEC input file appears in Figure 2.

Runs were made using the profile exponent values in Figure 1, and the corresponding loading profiles are plotted in Figure 3. The heaviest loading is the full WK profile corresponding to $\nu = 1$. The resistor in the first segment has a value of 45.2 Ω, while the last segment at the top of the monopole is loaded with 1220 Ω. Corresponding values for the least heavily loaded profile, $\nu = 0.05$, are 0.27 Ω and 461.4 Ω Interestingly, the loading resistance increases with increasing profile exponent at all segments except the last where the three highest resistances in increasing order correspond to ν values of 1, 0.8, and 0.4. But for all values of ν the data reflect the typical characteristic of progressively increasing resistance with distance from the RF source as seen in [1, 3–8]. As will be seen below, however, monotonically increasing profiles are not necessarily the best.

Figures 4 and 5 plot the monopole's input resistance and reactance. As for all plots in this paper, calculated data points are marked by symbols, and the continuous curves connecting data points have been interpolated using a natural cubic spline. As expected, excursions in the antenna's input impedance increase with decreasing profile exponent. The most heavily loaded profiles, $\nu = 1, 0.8,$

```
CM  Loaded Base-Fed Monopole on Perfect Ground
CM
CM      Monopole Height    =       10.668 meters
CM      Element Diameter   =        5.080 centimeters
CM      Design Frequency   =        7.028 Mhz
CM      Power-Law Exponent =        0.400
CM      Number of Segments =          14
CM
CM      Reactive Loading?      NO
CM
CM      Expansion Parameter:
CM      Re(Psi)=10.169, Im(Psi)=-2.431, Mag(Psi)=10.456
CM
CM      Run ID: 02-02-2011  14:55:38
CE
GW1,14,0.,0.,0.,0.,0.,10.668,.0254
GE1
LD0,1,1,1,4.676104,0.,0.
LD0,1,2,2,5.307981,0.,0.
LD0,1,3,3,6.091182,0.,0.
LD0,1,4,4,7.080875,0.,0.
LD0,1,5,5,8.360775,0.,0.
LD0,1,6,6,10.06334,0.,0.
LD0,1,7,7,12.40921,0.,0.
LD0,1,8,8,15.79046,0.,0.
LD0,1,9,9,20.96459,0.,0.
LD0,1,10,10,29.57042,0.,0.
LD0,1,11,11,45.77719,0.,0.
LD0,1,12,12,83.26774,0.,0.
LD0,1,13,13,214.1414,0.,0.
LD0,1,14,14,1983.914,0.,0.
GN1
FR 0,26,0,0,5.,1.
EX 0,1,1,1,1.,0.
RP 0,10,1,1001,0.,0.,10.,0.,100000.
EN
```

Figure 2. Extended loading profile NEC input file for $\nu = 0.4$.

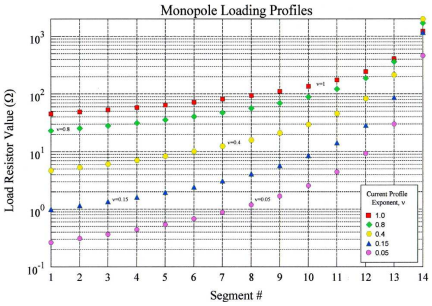

Figure 3. Discrete extended theory loading profiles.

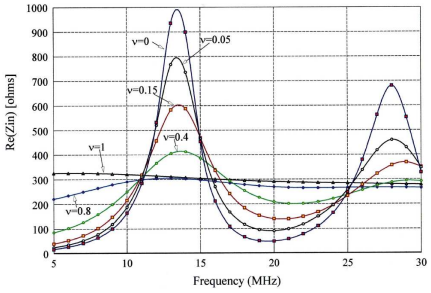

Figure 4. Loaded monopole input resistance.

show the flattest responses, especially for the input resistance. For comparison, the input impedance of the antenna with no loading ("metallic" monopole, $\nu = 0$) is plotted as well, and, of course, it exhibits the greatest variability.

Radiation efficiency appears in Figure 6. The effect of the profile exponent is dramatic. At 5 MHz, for example, the heavily loaded WK profile with $\nu = 1$ results in an efficiency of less than 4%, while the very light loading profile $\nu = 0.05$ increases it to nearly 70%. As with

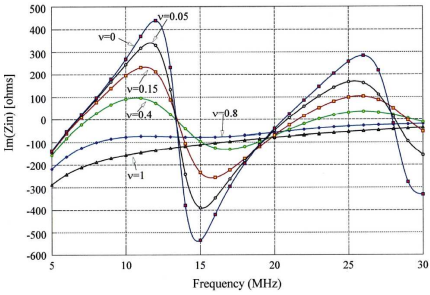

Figure 5. Loaded monopole input reactance.

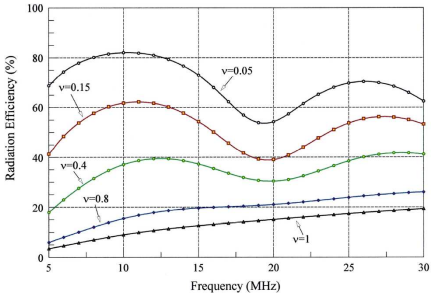

Figure 6. Loaded monopole radiation efficiency.

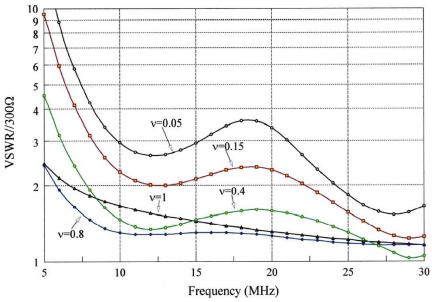

Figure 7. Loaded monopole VSWR//300 Ω.

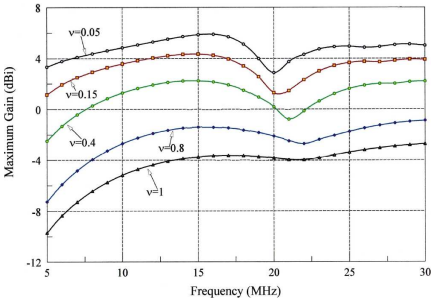

Figure 8. Loaded monopole maximum power gain.

the input impedance, lower values of profile exponent result in greater variability with frequency. At any given frequency, efficiency increases with decreasing exponent values.

Figure 7 plots the loaded monopole's VSWR versus frequency assuming a 300 Ω feed system characteristic impedance (the value used in [5]). As expected, the flattest response is achieved with the heaviest loading. But, somewhat surprisingly, the $\nu = 0.8$ curve is consistently better than the $\nu = 1$ curve. Compared to the full WK profile, the $\nu = 0.8$ profile provides both better radiation efficiency and VSWR performance. Profiles with $\nu = 0.4,\ 0.15,\ 0.05$, in that order, result in higher and more variable VSWR's. The profile with $\nu = 0.4$ provides what likely is the best tradeoff between VSWR and radiation efficiency. Loading at this level results in radiation efficiencies between about 18% and 41% with a VSWR below 2 : 1 at all frequencies above approximately 8 MHz without any matching network. Between 5 and 8 MHz the VSWR decreases quickly from approximately 4.6 : 1 to 2 : 1. As a general proposition, matching VSWR levels up to 10 : 1

in a fairly narrow band is readily accomplished with a simple, low-loss network. But because some matching must be done for each profile, the $\nu = 0.15$ profile may in fact be the best because it provides much higher efficiencies, between about 39% and 62%, with a maximum VSWR below 10 : 1 that falls quickly to approximately 2.5 : 1 at 10 MHz and thereafter remaining below that level.

Maximum power gain (product of directive gain and radiation efficiency) and radiation patterns for the loaded monopole appear in Figures 8 and 9, respectively. Gain was computed at 10° increments in the polar angle $0° \leq \theta \leq 90°$ in NEC's standard right-handed polar coordinate system. The maximum gain value over these angles is plotted. Gain increases with lighter loading, as expected, and the penalty paid for heavy loading is substantial. At 5 MHz, for example, the $\nu = 1$ profile's gain just above -10 dBi is more than 13 dB below the gain with $\nu = 0.05$ loading. The gap generally narrows with increasing frequency, but it remains significant across the HF band, greater than 7 dB or so.

The radiation patterns, which were computed at 1° increments in θ, show generally smooth variations without a great deal of lobing. Note that $\theta = 0°$ is in the direction of the zenith and $\theta = 90°$ the horizon, so that moderate take-off angles for long-distance links generally are in the range $60° \leq \theta \leq 80°$. In all cases the pattern is smoothest at 5 MHz. More scalloping develops with increasing frequency at all loading levels, and at a given frequency with lighter loading. As a reference, patterns for the unloaded metallic monopole are included, and, as expected, they show the greatest lobing. The gains with $0.05 \leq \nu \leq 0.4$ over angles of interest are for the most part comparable, and there is no clear basis for selecting one loading profile over another. The heavier loading profiles, by contrast, exhibit substantially lower gains and consequently are less desirable.

5. LOADED HF MONOPOLE USING NUMERICAL PROFILE

This section describes a numerical technique for computing an optimized loading profile using Central Force Optimization (CFO). CFO is a deterministic metaheuristic for global search and optimization that has been applied to problems in applied electromagnetics and tested against recognized benchmark suites [20–34]. While more efficient versions of the algorithm have been implemented recently on a GPU using multiple topologies (contact author for details), the parameter-free implementation described in [20] was used to determine an optimized loading profile for the RD HF monopole discussed in §4

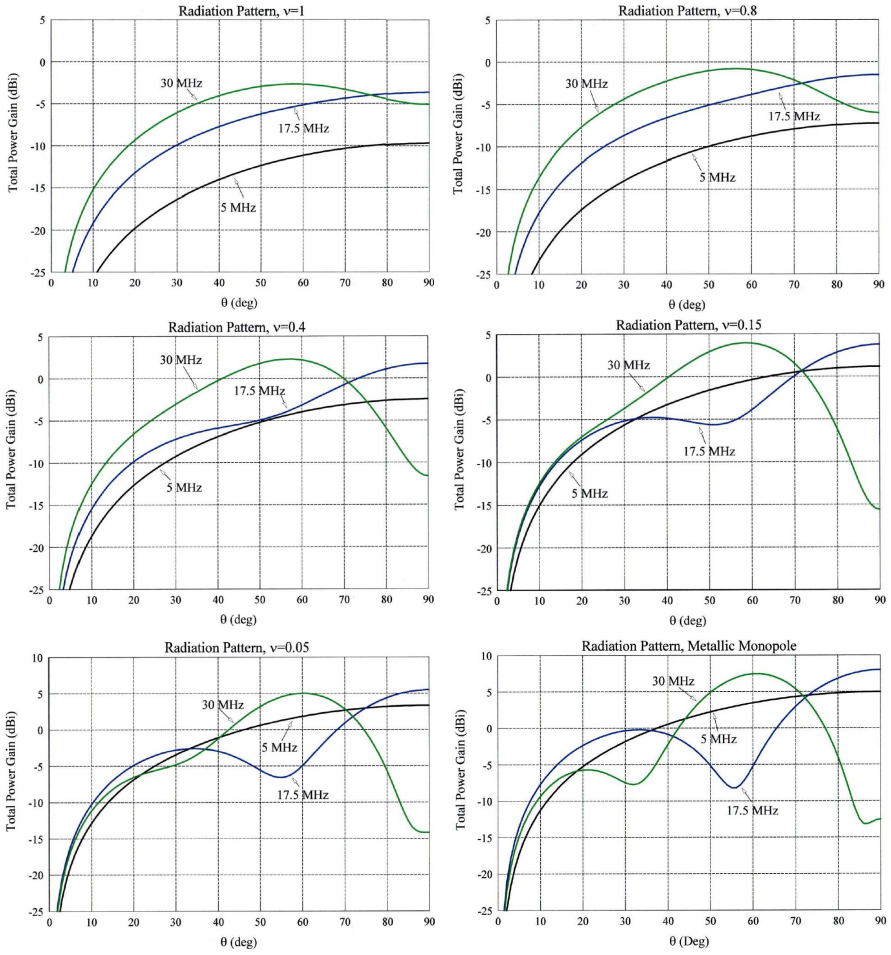

Figure 9. Loaded monopole radiation patterns.

(see also [23]).

The objective function being maximized is $f(R_L)=\frac{\min(\varepsilon)+\min(G_{\max})}{\Delta VSWR^{2.5}}$ where $R_L = (R_L^1, R_L^2, \ldots, R_L^{14})$ is the vector of load resistor values segment-by-segment along the monopole. The feasible space (allowable solutions) was $0 \leq R_L^k \leq 1000\,\Omega$, $k = 1, \ldots, 14$, chosen because analytical results suggest that maximum required load resistances are on the order of several hundred ohms. Of course, the decision space may be expanded or contracted based on many factors, for example, previous experience, data suggesting regions of "good" solutions (for

example, an analytical profile from §4), a "best guess," or practical constraints related to fabricating the antenna. The decision space size influences how well CFO or other optimizers work, which consequently also may be a factor in its specification.

$f(R_L)$'s functional form was chosen to return greater values for loading profiles that result in greater gain and efficiency and reduced variability in VSWR. $\min(\varepsilon)$ is the minimum radiation efficiency across the 5–30 MHz band (computed every 1 MHz), while $\min(G_{\max})$ is the corresponding minimum value of maximum total power gain. $\Delta VSWR$ is the difference between maximum and minimum VSWR relative to a feed system characteristic impedance $Z_0 = 300\Omega$. The exponent of 2.5 for this term was chosen empirically.

Of course, other functional forms could be used that might provide even better results. For example, a more general form than the one above is $f(R_L) = \frac{c_1 \cdot \min(\varepsilon) + c_2 \cdot \min(G_{\max})}{\Delta VSWR^{c_3}}$, which provides greater flexibility by including three user-specified constants, c_1, c_2, c_3. A still more general form might contain coefficients and exponents that are frequency-dependent, $c_i(f_{MHz})$, in order to improve performance in certain frequency ranges. Other functional forms could be used that reflect a completely different balance between the monopole's various performance measures.

One of CFO's major advantages over other optimizers is its determinism. Every CFO run with the same setup parameters yields the same results, in contrast to inherently stochastic optimizers that yield different outcomes on successive runs. In addition, many optimization algorithms require the user to provide several parameters specific to the algorithm, whereas CFO can be implemented parameter-free so that the only user input is the objective function to be maximized.

For "real world" problems such as the loaded monopole design, CFO allows the user to focus on the more important issues of the objective function's form and its parameter values. Because only one CFO run is required, the effects of changing the objective function's form or parameter values can be investigated directly, which cannot be done with a stochastic optimizer whether or not it requires user-input parameters. The decision space's topology is determined by the objective function's form and parameter values, and changing any of these changes the topology being searched. In general there is no way to know which topology actually produces the "best" antenna design. Even when the optimizer accurately locates the global maxima for a particular topology, it is entirely possible, even likely, that some other decision space may yield a better antenna. This question is more easily addressed with a deterministic optimizer such as CFO than it is with

a stochastic optimizer whose results never are the same.

The CFO optimization run reported here employs the parameter-free implementation described in [20] with directional information included in errant probe repositioning described in [31] and the following hard-wired parameter values: $F_{rep}^{init} = 0.5$, $\Delta F_{rep} = 0.1$, $\gamma_{start} = 0$, $\gamma_{stop} = 1$, $\Delta\gamma = 0.1$, $N_d = 14$, $(N_p/N_d)_{\max} = 4$, $N_t = 120$. Pseudocode appears in Figure 10. Readers wishing to implement their own versions of the program are advised to consult [20] for additional information that is beyond the scope of this paper.

Evolution of the optimizer's best fitness (objective function value), average probe distance (D_{avg}), and CFO's best probe number are

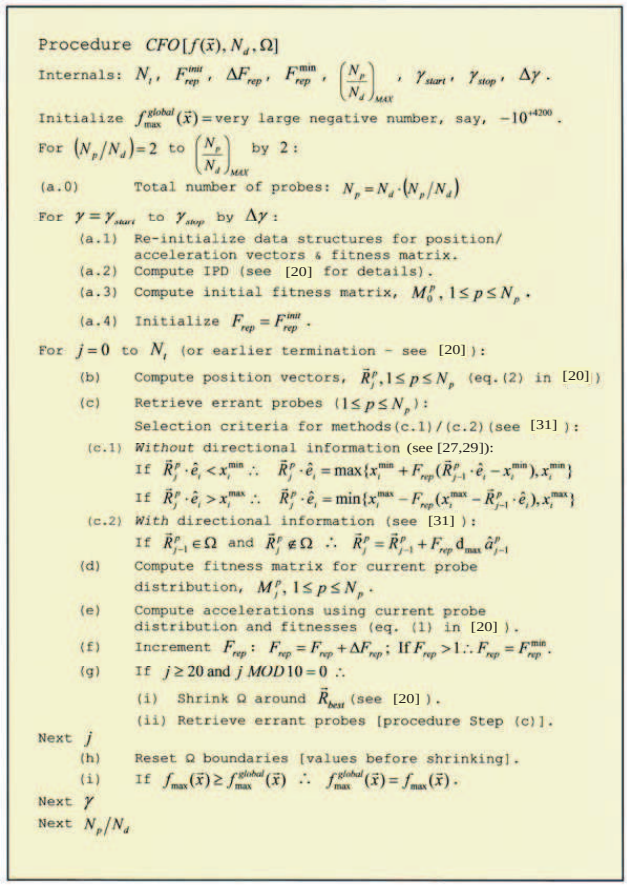

Figure 10. Parameter-free CFO Pseudocode (Ω is the decision space).

plotted in Figures 11–13, respectively. The fitness exhibits five main plateaus with three smaller (shorter duration) ones. This type of behavior has been seen in other antenna related problems, and may be characteristic of antenna decision spaces (see, for example, [23, 25]). D_{avg} is the average distance step-by-step between CFO's probe with the best fitness and all other probes. D_{avg} decreases as probes cluster around the global maximum, approaching zero as all probes coalesce onto the maximum. The best probe number plot shows how the probe returning the best fitness changes throughout a run. These plots and their significance are discussed at length in [20].

The CFO-optimized loading profile is shown in Figures 14 and 15. Figure 14 tabulates where each loading resistor is placed along the monopole's height and its value, while Figure 15 plots the resistance as a function of segment number. These figures are interesting because the numerically optimized profile is quite different than the profiles computed using the original WK theory or the extension developed in this paper.

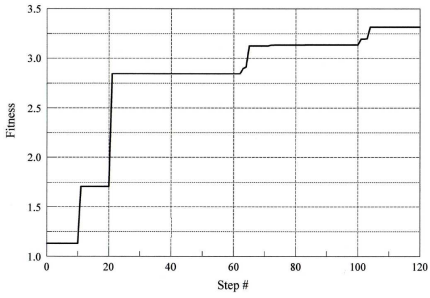

Figure 11. CFO best fitness.

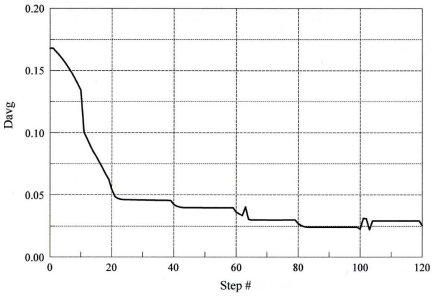

Figure 12. CFO D_{avg}.

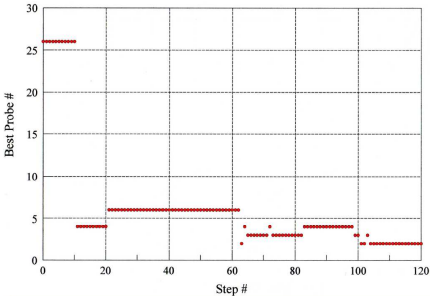

Figure 13. CFO best probe number.

Height (meters)	Resistance (Ω)
0.381	82.7045
1.143	29.3115
1.905	9.2825
2.667	7.1540
3.429	7.3978
4.191	7.3102
4.953	27.5870
5.715	26.5575
6.477	24.7010
7.239	22.8015
8.001	20.8245
8.763	16.4492
9.525	11.4537
10.287	9.4720

Figure 14. CFO-optimized loading profile.

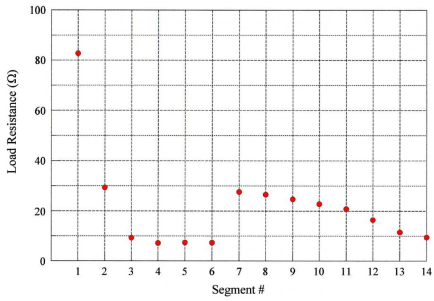

Figure 15. CFO-optimized monopole loading profile.

```
CM File: LD_MONO.NEC
CM Run ID 02-16-2011 10:43:46
CM Nd= 14, p= 2, j= 120
CM Zo=300 ohms
CE
GW1,14,0.,0.,0.,0.,0.,10.668,.0254
GE1
LD0,1,1,1,82.7045,0.,0.
LD0,1,2,2,29.31145,0.,0.
LD0,1,3,3,9.2825,0.,0.
LD0,1,4,4,7.154042,0.,0.
LD0,1,5,5,7.397769,0.,0.
LD0,1,6,6,7.310225,0.,0.
LD0,1,7,7,27.58697,0.,0.
LD0,1,8,8,26.55749,0.,0.
LD0,1,9,9,24.70102,0.,0.
LD0,1,10,10,22.80148,0.,0.
LD0,1,11,11,20.82445,0.,0.
LD0,1,12,12,16.44918,0.,0.
LD0,1,13,13,11.4537,0.,0.
LD0,1,14,14,9.471994,0.,0.
GN1
FR 0,26,0,0,5.,1.
EX 0,1,1,1,1.,0.
RP 0,10,1,1001,0.,0.,10.,0.,100000.
EN
```

Figure 16. CFO-optimized NEC input file.

In those profiles the loading resistance increases monotonically with increasing distance from the excitation point. The CFO profile, in marked contrast, starts with a high resistance that decreases approximately monotonically over about half the monopole height, then jumps to a higher value and thereafter continues to decrease monotonically. This behavior is quite different from the analytic profiles, and shows clearly that the WK theory and its extension are not a complete solution to the problem of creating travelling wave-only current modes using impedance loading.

Figure 16 shows the CFO-optimized monopole's NEC input file, and Figures 17–21 plot the NEC-2D results. The input resistance varies gradually with frequency from about $175\,\Omega$ to $575\,\Omega$, and the reactance exhibits a similar variation between approximately $-220\,\Omega$ and $+120\,\Omega$. These variations are moderate and should be expected to

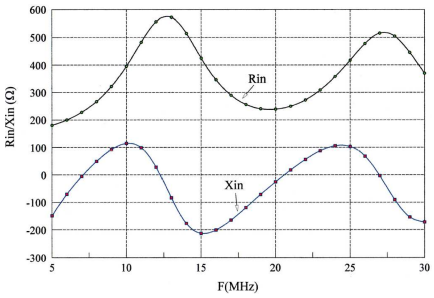

Figure 17. CFO loaded monopole input impedance.

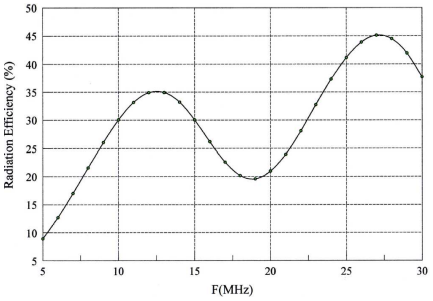

Figure 18. CFO loaded monopole radiation efficiency.

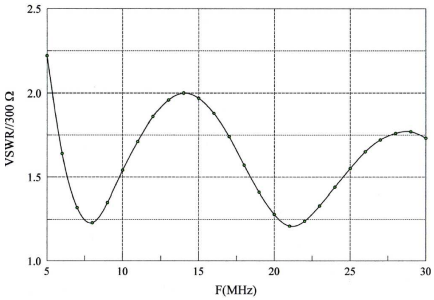

Figure 19. CFO Loaded Monopole VSWR//300 Ω.

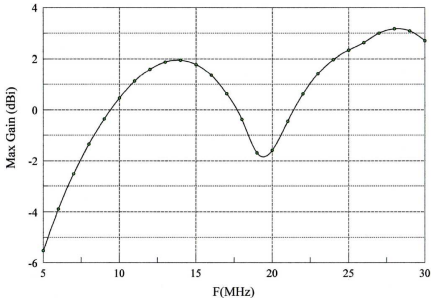

Figure 20. CFO loaded monopole maximum gain.

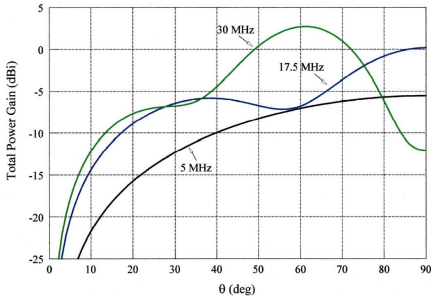

Figure 21. CFO loaded monopole radiation pattern.

result in a similarly moderate VSWR variation. Four resonant points ($X_{in} = 0$) appear below approximately 7.5, 15, 21 and 27.5 MHz at alternate resonances and anti-resonances in the monopole structure.

Figure 18 plots the monopole's radiation efficiency which ranges from a low of about 9% to a maximum of 45%. The worst efficiency

occurs at the lowest frequency, 5 MHz, as expected; but it increases quickly to about 15% near 7 MHz. Thereafter it exhibits an oscillatory behavior with a minimum slightly less than 20% near 19 MHz. The radiation efficiency of the CFO-optimized monopole is comparable to that using the analytically computed profiles discussed in §4.

Perhaps the most important single measure of the loaded monopole's effectiveness is its VSWR, which is plotted in Figure 19. VSWR//300 Ω is below 2 : 1 at all frequencies above approximately 5.3 MHz. Maximum VSWR is about 2.2 : 1 at 5 MHz. Thus, the CFO optimized monopole meets the standing wave ratio design objective essentially across the entire 5–30 MHz HF band without any matching network, which is quite significant because none of the analytic loading profiles performs as well. The CFO-optimized antenna is simpler, uses lower value resistance, does not require a continuously varying profile, and avoids the insertion losses inherent in any matching network.

The final measures of the CFO-optimized monopole's effectiveness are its maximum gain and radiation patterns, which are plotted in Figures 20 and 21. These patterns are similar to those produced by the analytic profiles.

6. CONCLUSION

This paper has presented two new approaches to broadbanding wire antennas using impedance loading: (1) an analytic method based on extending the seminal Wu-King theory for the internal impedance profile that produces purely travelling wave current modes; and (2) a numerical method based on the deterministic metaheuristic Central Force Optimization. The extended analytic profiles provide results generally better than the full or fractional WK profiles, and the CFO-optimized loading profile is better yet. These new techniques, especially CFO, should be useful in any broadband antenna design that incorporates impedance loading. CFO source code and any papers not freely accessible online are available upon request to the author (rf2@ieee.org).

REFERENCES

1. Willoughby, E. O., "An improved wide band aerial," *Patent Specification*, No. 162009, Commonwealth of Australia, Aug. 13, 1953.
2. Altshuler, E. E., "The traveling-wave linear antenna," *IRE Transactions on Antennas and Propagation*, 324, Jul. 1961.
3. Wu, T. T. and R. W. P. King, "The cylindrical antenna with nonreflecting resistive loading," *IEEE Transactions on Antennas*

and Propagation, 369–373, May 1965, (see also Corrections, *IEEE Trans. Ant. Prop.*, 998, Nov. 1965).

4. Kanda, M., "Time domain sensors for radiated impulsive measurements," *IEEE Transactions on Antennas and Propagation*, 438, May 1983.
5. Rama Rao, B. and P. S. Debroux, "Wideband HF monopole antennas with tapered resistivity loading," *IEEE Military Communications Conference*, Monterey, CA, Sep. 30–Oct. 3, 1990.
6. Rama Rao, B., "Optimized tapered resistivity profiles for wideband HF monopole antenna," *IEEE Ant. & Prop. Soc. Symposium*, London, Ontario, Canada, 1991.
7. Little, L., O. Ramabi, and R. Mittra, "Combined tapered resistive and inductive loading to increase the bandwidth of small antennas," *Proceedings of the IEEE Ant. & Prop. Soc. Symposium*, 2089, Jul. 1992.
8. Lestari, A. A., E. Bharata, A. B. Suksmono, A. Kurniawan, A. G. Yarovoy, and L. P. Ligthart, "A modified bow-tie antenna for improved pulse radiation," *IEEE Transactions on Antennas and Propagation*, 2184–2192, Jul. 2010.
9. King, R. W. P., G. J. Fikioris, and R. B. Mack, *Cylindrical Antennas and Arrays*, Cambridge University Press, New York, USA, 2002.
10. Valagiannopoulos, C. A., "Electromagnetic scattering of the field of a metamaterial slab antenna by an arbitrarily positioned cluster of metallic cylinders," *Progress In Electromagnetics Research*, Vol. 114, 51–66, 2011.
11. Valagiannopoulos, C. A. and G. Fikioris, "On choosing kernel and feed when analyzing dipole antennas via integral equations," *10th International Conference on Mathematical Methods in Electromagnetic Theory, Conference Proceedings*, 257–259, Dniepropetrovsk, Ukraine, Sep. 14–17, 2004.
12. Fikioris, G. and C. A. Valagiannopoulos, "Input admittances arising from explicit solutions to integral equations for infinite-length dipole antennas," *Progress In Electromagnetics Research*, Vol. 55, 285–306, 2005.
13. Abramowitz, M. and I. Stegun, *Handbook of Mathematical Functions with Formulas, Graphs, and Mathematical Tables*, Ninth Printing, 231, US Department of Commerce, National Bureau of Standards Applied Mathematics Series 55 (AMS 55), Nov. 1970.
14. Formato, R. A., "Loading profiles for wideband antennas,"

Communications Quarterly Magazine, 27, Summer 1997, (see also Corrections, 93, Fall 1997).

15. Formato, R. A., "Wideband antennas," *Electronics World Magazine*, 202, Mar. 1997.
16. Formato, R. A., "Maximizing the bandwidth of monopole antennas," *NARTE News*, Vol. 11, No. 4, 5, National Association of Radio and Telecommunications Engineers, Inc., Oct. 1993–Jan. 1994.
17. (i) 4nec2 Antenna Modeling Freeware by A. Voors, available online at http://home.ict.nl/∼arivoors/. (ii) Unofficial Numerical Electromagnetic Code (NEC) Archives, online at http://www.si-list.net/swindex.html.
18. Burke, G. J. and A. J. Poggio, "Numerical electromagnetics code (NEC) — Method of moments," Parts I, II and III, UCID-19934, Lawrence Livermore National Laboratory, Livermore, California, USA, Jan. 1981.
19. Burke, G. J., "Numerical electromagnetics code — NEC-4, method of moments, Part I: User's manual and Part II: Program description — Theory," UCRL-MA-109338, Lawrence Livermore National Laboratory, Livermore, California, USA, Jan. 1992, https://ipo.llnl.gov/technology/software/softwaretitles/nec.php.
20. Formato, R. A., "Parameter-free deterministic global search with simplified central force optimization," *Proceeding ICIC'10 Proceedings of the 6th International Conference on Advanced Intelligent Computing Theories and Applications: Intelligent Computing* , 309–318, Springer-Verlag, Berlin, Heidelberg, 2010.
21. Cross, M. W., E. Merulla, and R. A. Formato, "High-performance indoor VHF-UHF antennas: Technology update report," National Association of Broadcasters (NAB), FAS-TROAD (Flexible Advanced Services for Television and Radio On All Devices), Technology Advocacy Program, May 15, 2010, http://www.nabfastroad.org/NABHighperformanceIndoorTVantennaRpt.pdf.
22. Qubati, G. M., N. I. Dib, and R. A. Formato, "Antenna benchmark performance and array synthesis using central force optimization," *IET (UK) Microwaves, Antennas & Propagation*, Vol. 4, No. 5, 583–592, 2010, doi: 10.1049/iet-map.2009.0147.
23. Formato, R. A., "Improved CFO algorithm for antenna optimization," *Progress In Electromagnetics Research B*, 405–425, 2010, http://www.jpier.org/pierb/pier.php?paper=09112309, doi:10.2528/PIERB09112309.
24. Formato, R. A., "Central force optimization and NEOs — First

cousins?," *Journal of Multiple-valued Logic and Soft Computing*, Vol. 16, 547–565, 2010.

25. Formato, R. A., "Central force optimization applied to the PBM suite of antenna benchmarks," 2010, arXiv:1003.0221, http://arXiv.org.
26. Xie, L., J. Zeng, and R. A. Formato, "Convergence analysis and performance of the extended artificial physics optimization algorithm," *Applied Mathematics and Computation*, 2011, online at http://dx.doi.org/10.1016/j.amc.2011.02.062.
27. Formato, R. A., "Central force optimisation: A new gradient-like metaheuristic for multidimensional search and optimisation," *Int. J. Bio-inspired Computation*, Vol. 1, No. 4, 217–238, 2009, doi: 10.1504/IJBIC.2009.024721.
28. Formato, R. A., "Central force optimization: A new deterministic gradient-like optimization metaheuristic," *Journal of the Operations Research Society of India*, Vol. 46, No. 1, 25–51, 2009, doi: 10.1007/s12597-009-0003-4.
29. Formato, R. A., "Central force optimization: A new computational framework for multidimensional search and optimization," *Nature Inspired Cooperative Strategies for Optimization (NICSO 2007)*, N. Krasnogor, G. Nicosia, M. Pavone, and D. Pelta, Eds., Vol. 129, Springer-Verlag, Heidelberg, 2008.
30. Formato, R. A., "Central force optimization: A new metaheuristic with applications in applied electromagnetics," *Progress In Electromagnetics Research*, Vol. 77, 425–491, 2007.
31. Formato, R. A., "On the utility of directional information for repositioning errant probes in central force optimization," 2010, arXiv:1005.5490, http://arXiv.org.
32. Formato, R. A., "Pseudorandomness in central force optimization," 2010, arXiv:1001.0317, http://arXiv.org.
33. Formato, R. A., "Are near earth objects the key to optimization theory?" 2009, arXiv:0912.1394, http://arXiv.org.
34. Formato, R. A., "Issues in antenna optimization — A monopole case study," Mar. 2011, http://arXiv.org/abs/1103.5629.